sustainability

MDPI

Article

Experimental Analysis of the Effect of Geometry and Façade Materials on Urban District's Equivalent Albedo

Elena Morini, Beatrice Castellani *, Andrea Presciutti, Elisabetta Anderini, Mirko Filipponi, Andrea Nicolini and Federico Rossi

Engineering Department, Interuniversity Research Centre on Pollution and Environment "Mauro Felli" (CIRIAF), University of Perugia, Via G. Duranti 67, 06125 Perugia, Italy; morini@crbnet.it (E.M.); andrea.presciutti@unipg.it (A.P.); anderini.unipg@ciriaf.it (E.A.); filipponi.unipg@ciriaf.it (M.F.); andrea.nicolini@unipg.it (A.N.); federico.rossi@unipg.it (F.R.)

* Correspondence: beatrice.castellani@unipg.it; Tel.: +39-0755853853

Received: 26 May 2017; Accepted: 12 July 2017; Published: 16 July 2017

Abstract: Urban Heat Island (UHI) is influenced by urban form, geometry, and the properties of surfaces. Retroreflective (RR) materials have been proposed as a countermeasure to UHI, thanks to their optical property of reflecting most of the incident solar energy back towards the same direction. In this paper, the effect of RR materials on urban districts was investigated. They were applied on building façades of urban districts with different urban forms and orientations. To this aim, an experimental model resembling urban districts with different geometries was built and RR materials on vertical surfaces were tested and compared to conventional construction materials with similar global reflectance. The trend of the instantaneous albedo was monitored during the day and a new parameter called "equivalent albedo" was used to demonstrate the effectiveness of the RR materials. The comparative analysis shows that the RR façades lead to an increase of the equivalent albedo for all of the investigated urban patterns. For a block pattern, the equivalent albedo increase is equal to 3%, while for canyon patterns it is equal to 7%. Results of energy evaluations show that the energy savings obtainable with the use of RR materials is comparable to the values of anthropogenic heat emissions in residential areas.

Keywords: urban heat island; urban district; retroreflective materials; equivalent albedo

1. Introduction

The Urban Heat Island (UHI) effect is a phenomenon that occurs in urban areas. It is due to build environment and human activities that make cities several degrees warmer than rural and suburban areas [1]. The UHI intensity is mainly due to human modification of the atmospheric environment [2–4]. UHI is influenced by several factors, including lower evaporation, increasing anthropogenic heat, lower air circulation in urban canyons, more pollutants in the atmosphere, topography, city size, low albedo, high heat capacity, and decrease in evapotranspiration [5–7].

Several studies found that the increased urban temperatures heavily impact the energy consumption of buildings during the summer period, affect human health [8], deteriorate indoor and outdoor thermal comfort [9,10], raise the concentration of harmful pollutants [11,12] and increase the carbon footprint of urban facilities and utilities [13].

Strategies for UHI mitigation have been widely investigated, and cool roofs, cool pavements [14–17], and urban vegetation including roof gardens and wet roofs [18–20] have emerged as new materials for thermal energy storage [21]. Urban vegetation allows the modification of the heat balance of the city by evapotranspiration and by intercepting solar radiation. In particular, this aspect has been studied for Cairo's urban developmentsas a function of two parameters: leaf area index, LAI and leaf area density, LAD [19].

The energy saving potentials of cool roofs have been recognized; they can reduce cooling costs with a possible small increase in heating costs [22,23], they have a positive effect on the quality of life in urban areas [24,25], they can lead to an offsetting of CO_2 emissions [26–28], and they can be an effective strategy in cold regions as well [29–31]. Strong efforts have been made to investigate innovative cool materials such as retroreflective materials (RR) [32–34], thermo chromic pigments [35], and directional reflective materials [36].

As regards RR materials, previous experimental studies have focused on: (i) the analytical modelling of RR materials' behaviour for perpendicular incident radiation [37]; (ii) the evaluation of the optic properties of RR samples for several angles of incidence [38]; and (iii) the evaluation of RR cooling effect at the urban canyon level in terms of reduction of the energy circulating inside the canyon [39].

In particular, results show that RR materials reflect the incident radiation mainly back toward the incoming direction for low incidence angles, while they lose this property for high incidence angles [40]. The distribution of reflected radiation by a diffusive material follows the Lambert law:

$$W_{r,\alpha} = \frac{W_i \cdot r}{\pi} \cos\alpha \tag{1}$$

Measurement results of previous studies [40] demonstrated that the angular distribution of the reflected radiation by a retroreflective surfaces depends on cos$n$, where "n", which depends on the material, represents a "concentration factor" of the reflected radiation around the direction of the incident radiation. The previous experimental campaigns have demonstrated the mitigation effects of RR materials in urban canyon scenarios [39,41].

Studies have analysed different strategies to introduce in urban planning tools in order to address climate change and subsequent risk disaster [42]. Generally, such instruments are based on three pillars: energy efficiency (EE), renewable energy sources (RES), and greenhouse gas emission reduction. In this context, solar energy technologies have already been presented as a good opportunity. Due to their demonstrated ability to reduce urban albedo and their cooling potential in terms of energy reflected and sent beyond the urban canyon [38], RR materials could also be considered a mitigation and adaptation strategy of climate change to add to the kit of urban planning tools.

The present paper aims to assesses the albedo change in an urban district physical model after the implementation of RR materials and as a function of urban geometry.

To this end, RR materials were tested and compared to conventional construction materials with similar global reflectance. The effect of both materials and urban patterns on the energy kept inside the urban canopy and thus on the heat island phenomenon was evaluated by introducing and calculating a new parameter, called "equivalent albedo" of an urban area.

The work is organized according to the following scheme: Section 2 introduces the materials and methods used for the experimental analysis; Section 3 shows the results and the discussion; conclusions are given in Section 4.

The results show that RR materials increase the equivalent albedo for all of the investigated urban patterns with a major effect on canyon schemes.

2. Materials and Methods

2.1. The Test Field

The experimental facility was located in Terni, on the roof of a building of the Applied Physics Department, University of Perugia. The considered urban geometries, orientations, and dimensions were taken from a previous study [41]. Concrete cubes of 15 cm sides were employed to reproduce urban scenarios with different geometries. The black membrane of the roofing material represents the bitumen of the street. The reproduced urban patterns are represented in Figure 1.

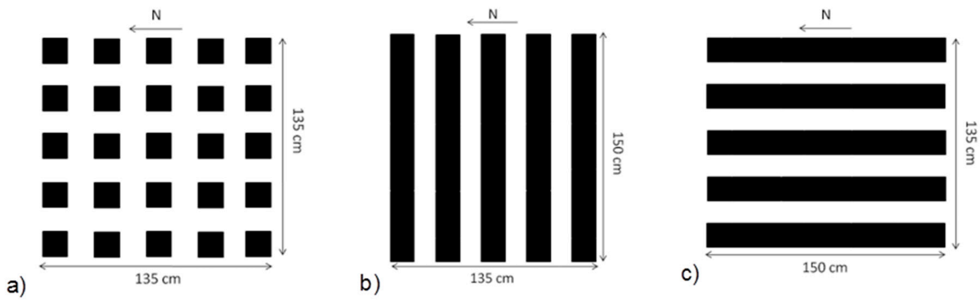

Figure 1. Schemes of the urban structure: (**a**) Blocks; (**b**) W-E canyons; (**c**) N-S canyons.

The urban districts analyzed could represent the scale model of real urban cities such as Athens (a) and New York (b,c). For these cities, the UHI exceeds 4° [43] and 8° [44] respectively. An in-depth weather analysis is provided in Reference [45,46].

In the blocks structure, the cubes were placed at a distance of 15 cm from each other. The outermost vertexes of the cubes at the corners form a square of 135 cm by 135 cm. In the W-E canyons, the cubes were placed in five rows with a distance between of 15 cm. The cubes disposed in this way formed four canyons in the West-East direction. The value of the H/D ratio that characterizes the canyons was 1. The outermost vertexes defined an area of 135 cm by 150 cm. In the N-S canyons, the cubes were in five rows, with 15 cm distance between each other, and formed four canyons in the North-South direction. The H/D ratio was 1. The occupied area was 150 cm by 135 cm. The facility was exposed to the sun from sunrise to sunset. The three configurations were designed to have the same exposed vertical surface inside the perimeter. To pursue this condition, referring to the schemes depicted in Figure 1, 25 blocks were installed in the urban structure (a) (block shape) and 50 blocks were installed in the urban structures (b,c) (W-E and N-S canyons).

For each scheme shown in Figure 1, measurements were carried out with two different materials: traditional concrete and retroreflective (RR) membrane [47]. Figure 2 shows the test fields with lateral surfaces covered with RR materials.

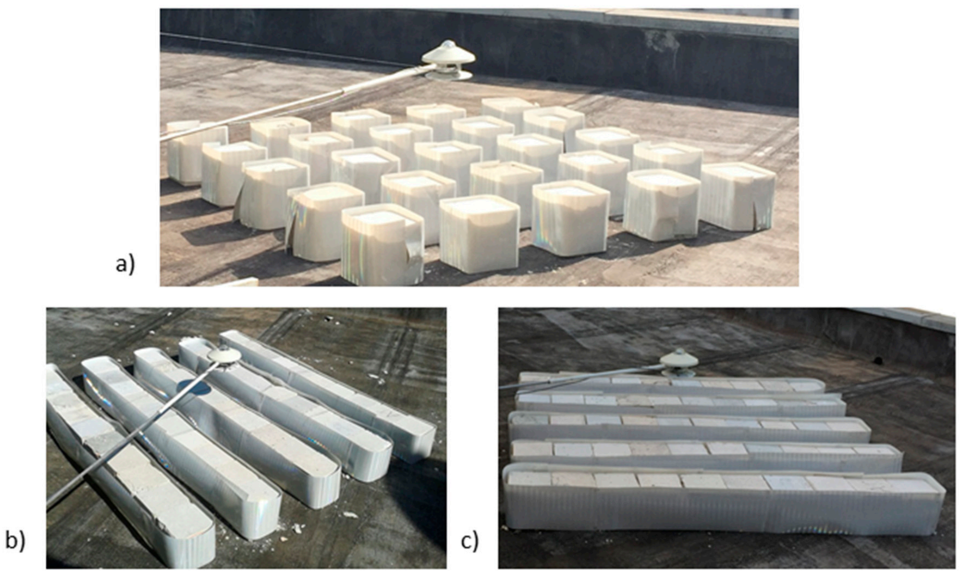

Figure 2. Schemes of the urban structure with RR lateral surfaces: (**a**) Blocks; (**b**) W-E canyons; (**c**) N-S canyons.

An albedometer, supplied by Delta Ohm Srl (model LP PYRA 05) and constituted by two pyranometers (Class I), was used to measure the albedo during the whole day. The albedo is calculated as the ratio between the reflected solar radiation and the diffuse radiation incident from the bottom hemisphere. The technical data of the sensors are provided in Reference [48].

In accordance with the procedure published in other works [41], it was positioned in a central position of each scheme, at a height of 30 cm above the blocks. It is close enough to the blocks to assess that the measured albedo is representative of the characteristic of the scheme, and albedo variations are due to the variations of the characteristics of the scheme (geometry and properties of materials). Measurements were carried out from 1 September to 10 September in accordance with the weather conditions required, which were clear sky conditions.

2.2. Optic-Energy Characterization of Materials

The solar reflectance of the blocks and the RR film was measured through a spectrophotometric analysis. The hemispherical spectral reflectance of the samples was measured using a Ultraviolet/Visible/Near Infrared (UV/VIS/NIR) by by Shimadzu Solid Spec 3700 spectrophotometer [49] equipped with 60 mm integrating sphere. The wavelength range of measurements was 280–2500 nm, which includes 99% of the solar energy. The solar reflectance of the samples was then calculated using the appropriate standards (ASTM Standard G 173 [50,51]). The investigated samples are shown in Figure 3.

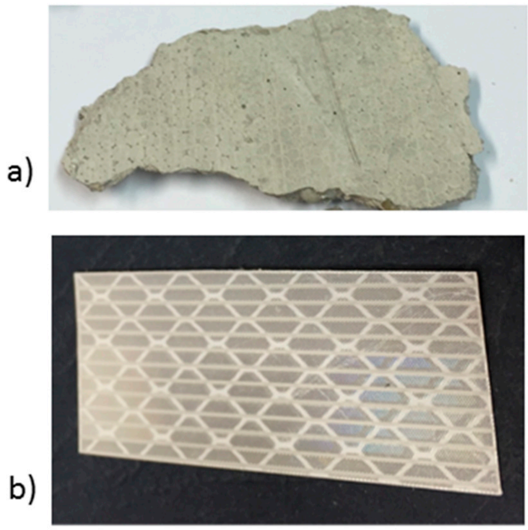

Figure 3. Investigated samples: (**a**) concrete sample; (**b**) RR sample.

Spectrophotometric analysis was carried out on one RR membrane sample and on five concrete samples (C1–C5), to take into account the effect of surface irregularity. The reflectance spectra of the samples are reported in Figure 4.

Concrete samples show very similar behavior. The RR sample shows higher values of reflectance between 400 nm and 600 nm, 900 nm and 1650 nm, and 1900 nm and 2100 nm, as well as lower reflectance values for the remaining intervals. According to the calculations, they show a comparable average total reflectance equal to 55% (55.048% for the C samples and 54.98% for the RR sample).

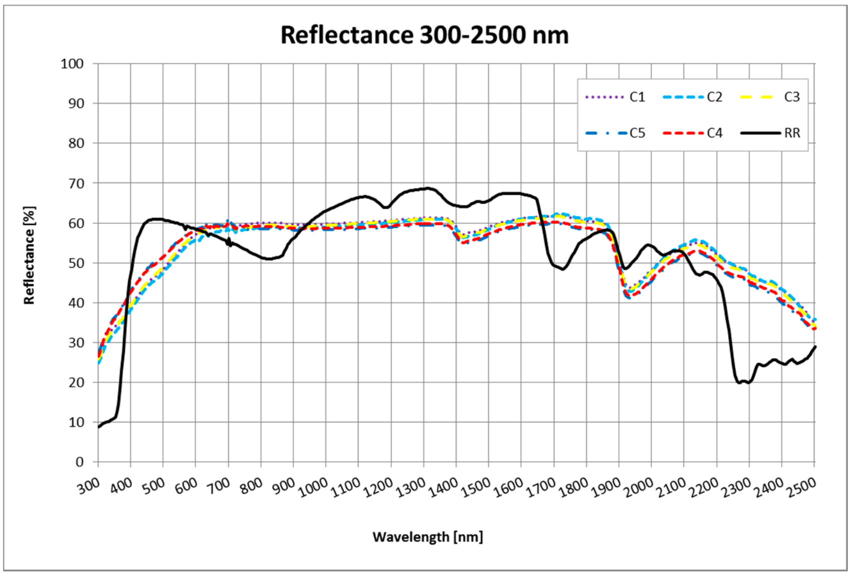

Figure 4. Reflectance spectra of the concrete samples C1, C2, C3, C4 and the RR film.

In accordance with procedure described in Reference [37], diffusive and RR samples were characterized in terms of angular distribution of the reflected energy (from −90° to 90°). The samples' behavior is graphed in Figure 5.

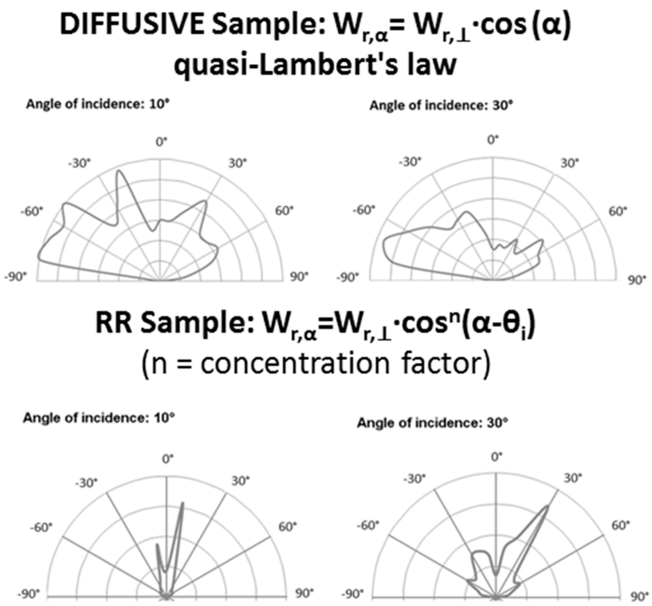

Figure 5. Angular distribution of reflected light: diffusive sample and RR sample [30].

With respect to the diffusive sample, the RR material has a predominant retroreflected component backward to the incoming direction.

3. Results and Discussion

A monitoring campaign during the first 10 days of September 2015 was carried out in the test facility for each scheme, with diffusive and RR materials. Daily albedo trends recorded during the day are shown in Figures 6–8. Each figure reports the monitored daily albedo values for the block scheme, W-E canyons, and N-S canyons, respectively. The considered time interval is the one that has the minimum cloud cover for all the schemes and conditions (from 7:20 to 16:40).

As regards the block scheme in Figure 6, the daily trend shows that the albedo in the presence of RR materials is higher with respect to the diffusive material during most of the day. Some slightly lower values can be found from 10:20 to 12:00 and at 15:45.

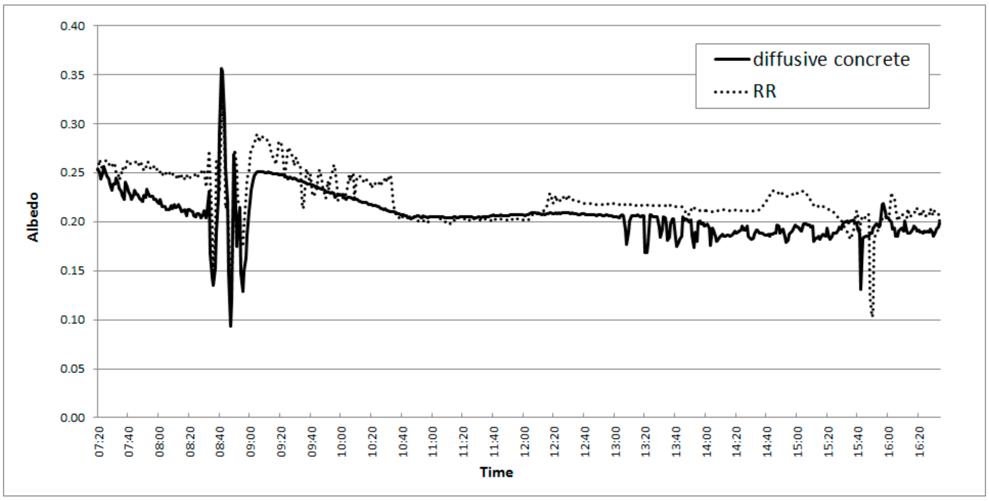

Figure 6. Daily albedo of the block shape scheme.

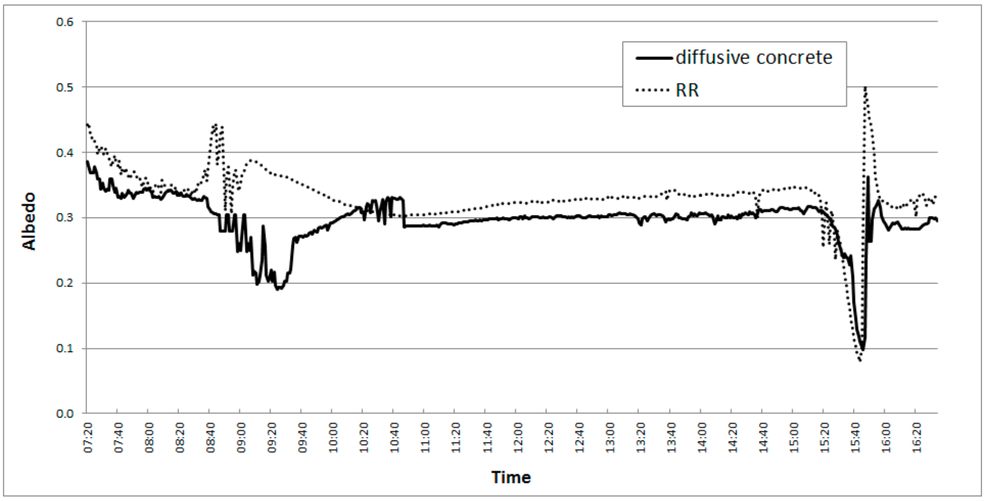

Figure 7. Daily albedo of the W-E canyons scheme.

Figure 7 shows the daily albedo results for the W-E canyons scheme. The measured albedo in the RR canyons is clearly higher than in the concrete canyons throughout the whole day. The maximum difference can be found in the morning, before 10:00. Then, in the central hours, a quite constant value of albedo for both the materials can be observed.

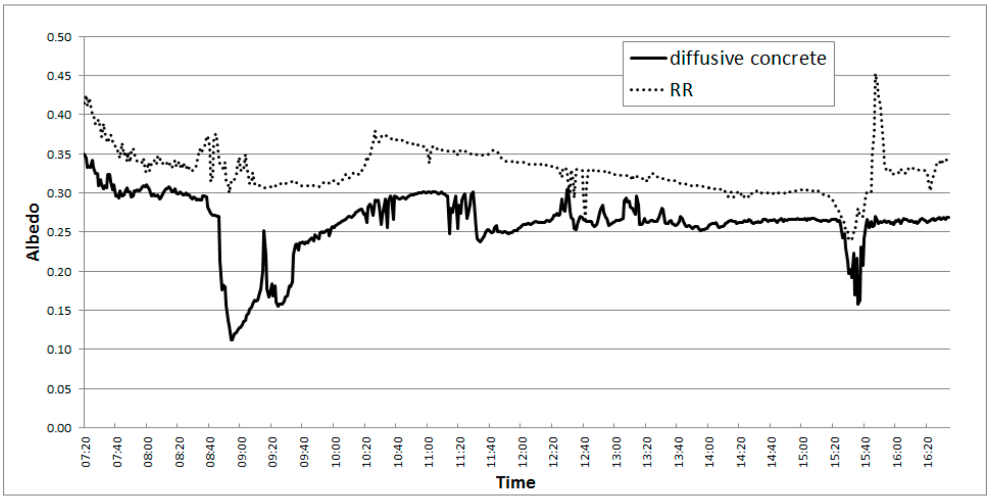

Figure 8. Daily albedo of the N-S canyons scheme.

Finally, Figure 8 depicts the trend of albedo for the N-S canyons scheme. In this configuration, the albedo in the presence of RR materials is clearly higher than the albedo with diffusive concrete.

This means that RR materials have a beneficial effect at each time of the day and allow energy saving within the urban form with a canyon structure. During the central hours of the day, in all the investigated patterns, the albedo is constant. In effect, at this time the sun is high and the incident radiation arrives perpendicular to the horizontal surfaces of the urban district. In the morning and in the afternoon, when solar radiation hits the surfaces with different inclinations, the instantaneous albedo profiles in all cases show sharp fluctuations, suggesting that urban albedo is a time-dependent parameter. It is in fact mainly influenced by the interaction between urban pattern and solar irradiation, which changes during the day. To take into account this aspect, which becomes crucial at an urban district level, a new parameter is here introduced and called "urban equivalent albedo". It is defined as the ratio between the reflected radiation and the solar incident radiation both integrated on the hemisphere and during the day, as shown in Equation (2).

$$\alpha_{EQ} = \frac{\int_0^{24} \int_0^{2\pi} W_r d\Omega dt}{\int_0^{24} \int_0^{2\pi} W_i d\Omega dt} \tag{2}$$

The equivalent albedo was calculated, in accordance with Equation (2), for the three schemes analyzed in the time interval from 07:20 to 16:40. Results are shown in Table 1. The daily albedo of the ground without blocks is 0.17. The presence of blocks (whose reflectance is about 55%, as stated before) causes an increase of albedo.

Table 1. Equivalent albedos and related % increase.

Scheme	Equivalentalbedo(Diffusive Concrete)	Equivalent Albedo(RR)	ΔAlbedo (%)
Blocks	0.21	0.24	+3%
W-E canyons	0.29	0.36	+7%
N-S canyons	0.28	0.35	+7%

There is an improvement in the equivalent albedo values due to the use of RR materials for all the schemes investigated; this is due to the directional properties of RR façades. In particular, for the block scheme, the daily equivalent albedo is 0.21 for diffusive concrete and 0.24 for RR materials, with an increase equal to 3%. For the W-E canyons scheme, the equivalent albedo passes from 0.29 to 0.36 with RR materials. The equivalent albedo in N-S canyons scheme passes from 0.28 to 0.35. The increase reaches 7% for both the canyon configurations.

Another consideration can be made on the basis of the results in Table 1. The equivalent albedo is affected by the urban pattern, with higher values in presence of canyon urban structures with respect to the block pattern. This is clearly shown in Figure 9, in which the instantaneous albedo values of the three schemes are compared (the first graph a) in presence of diffusive façades and the second graph b) with RR surfaces).

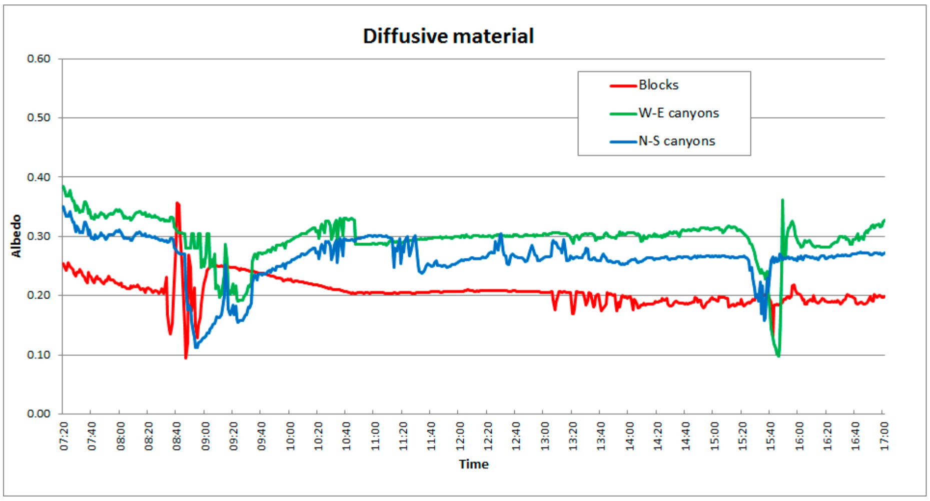

(**a**)

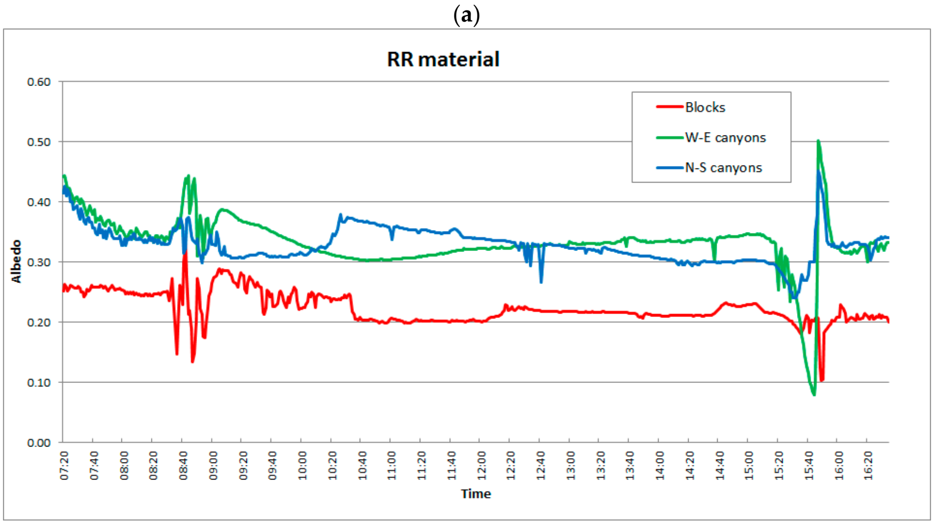

(**b**)

Figure 9. Daily instantaneous albedo: (**a**) Diffusive Materials, (**b**) RR Materials.

Canyon structures ensure higher albedo during the day than the block structure, in the presence of both diffusive and RR materials. Such a difference is mainly due to the number of concrete blocks that are positioned on the ground. In fact, to have the same exposed vertical surface on the three urban structures, 50 concrete blocks were needed for the block shape and 25 concrete blocks were instead used for the canyon structures.

This difference in the horizontal surface area, which represents the roofs of the urban district, causes different albedo values. In the presence of diffusive concrete façades, with respect to the block structure, the albedo increases by 7% with N-S canyons and 8% with W-E canyons. The directional property, i.e., the property to reflect the radiation back in the same direction of incidence, of the RR surface intensifies this effect.

The results show that, with an equal amount of exposed vertical surface area, the urban irregularity influences the equivalent albedo; if increasing the irregularity of the urban scheme, it is necessary to install more reflective materials on the vertical surfaces in order to have the same effect as that achieved in a more regular scheme.

The benefits obtained with the use of RR façades in terms of equivalent albedo of the considered urban district models lead to an improvement of the total amount of energy that is reflected outward from the urban canopy, thus reducing the energy circulating inside the urban volume.

According to the value of the annual average solar irradiation in a tropical city, Lao PDR [50] of about 16 MJ/m^2 day, the amount of energy saved with RR façades is indeed equal to: (i) 0.48 MJ/m^2 day, which is almost 50,000 MJ/day for a 100,000 m^2 district with the block structure; (ii) 1.12 MJ/m^2 day, which is more than 100,000 MJ/day for a 100,000 m^2 district with the canyon structure. Results of energy calculations are summarized in Table 2.

Table 2. Energy saving with RR façades in different urban patterns.

Urban Pattern	Solar Irradiation (MJ/m^{2}day)	ΔEquivalent Albedo	Energy Saving (MJ/m^2·day)
Blocks	16	0.03	−0.48
Canyons	16	0.07	−1.12

The energy savings, i.e., cooling potential of RR materials in terms of energy reflected and sent beyond the urban canyon (measured in this case in MJ/m^2 day) have been roughly calculated by considering an Δequivalent albedo equal to 0.03 and 0.07 as in Table 2, with a typical solar irradiation of 16 MJ/m^2·day and a 100,000 m^2 district.

The estimated energy saving obtainable with the use of RR materials is comparable to the values of anthropogenic heat emissions expressed in MJ/m^2·day for residential areas in tropical cities, as estimated [52].

Adhikari et al. [52] estimates the temporal variability of the anthropogenic heat flux density by separately considering the major sources of waste heat in urban environments, which include heat release from vehicular traffic, buildings, and human metabolism, respectively. The calculated anthropogenic heat flux density varies as a function of weekdays and study area, and ranges from 1.1 MJ/m^2·day to 7.5 MJ/m^2 day, which has a comparable order of magnitude of the hypothesized benefit above.

4. Conclusions

This paper investigates the influence of retroreflective materials on the albedo of experimental models resembling urban districts with different geometries. Three different geometries were investigated: a block structure, a West-East canyon structure, and a North-South canyon structure. For the three urban structures, the albedo was monitored during the day both in the presence of conventional diffusive building material and RR material. In addition, a new parameter called "urban equivalent albedo" is introduced to take into account the interaction between solar irradiation and urban pattern, which changes during the day. The comparative analysis shows that the RR façades lead to an increase of the equivalent albedo for all of the investigated urban patterns. This is due to the reflective properties of the RR membrane, which reflects the incident solar energy outward towards the same direction of incidence and thus does not diffuse the energy within the urban canopy. For the block structure, the equivalent albedo increase is equal to 3%, while for the canyon schemes the equivalent albedo increase is equal to 7%. It follows that a more irregular urban structure leads to the need for a more reflective material to gain the same albedo improvement as in a more regular urban scheme.

Energy evaluation shows that the estimated energy saving obtainable with the use of RR materials is comparable to the values of anthropogenic heat emissions in residential areas.

The present work focused on the analysis of the optic-energy properties of materials. As for future developments of the research, it will investigate how such properties can interact in the real scale, and the fluid dynamics of the setup will be studied to check the similitude with real-scale applications.

In effect, the obtained results in the small scale needed to be verified in real-scale applications in order to also consider the convective phenomena.

Further future studies will be focused on the relation between albedo and outdoor comfort by considering the connection between urban degree of compactness and equivalent albedo.

A future goal will also be the assessment of albedo-improvement costs in current cities.

Author Contributions: E.M., A.P., E.A. developed the experimental setup. E.M., B.C., A.P. and E.A. carried out the experimental campaign and analyzed data. E.M., B.C., E.A. wrote the paper. A.P., M.F. and A.N. contributed analysis tools. F.R. supervised the research activities.

Conflicts of Interest: The authors declare no conflict of interest.

References

1. Oke, T.R. The energetic basis of the urban heat island. *Q. J. R. Meteorol. Soc.* **1982**, *108*, 1–24. [CrossRef]
2. Oke, T.R. City size and the urban heat island. *Atmos. Environ.* **1973**, *7*, 769–779. [CrossRef]
3. Kalnay, E.; Cai, M. Impact of urbanization and land-use change on climate. *Nature* **2003**, *423*, 528–531. [CrossRef] [PubMed]
4. Wong, N.H.; Chen, Y. Study of green areas and urban heat island in a tropical city. *Habitat Int.* **2005**, *29*, 547–558. [CrossRef]
5. Oke, T.R.; Johnson, D.G.; Steyn, D.G.; Watson, I.D. Simulation of surface urban heat island under 'ideal' conditions at night—Part 2: Diagnosis and causation. *Bound.-Layer Meteorol.* **1991**, *56*, 339–358. [CrossRef]
6. Castellani, B.; Morini, E.; Filipponi, M.; Nicolini, A.; Palombo, M.; Cotana, F.; Rossi, F. Comparative Analysis of Monitoring Devices for Particulate Content in Exhaust Gases. *Sustainability* **2014**, *6*, 4287–4307. [CrossRef]
7. Touchaei, A.G.; Wang, Y. Characterizing urban heat island in Montreal (Canada)—Effect of urban morphology. *Sustain. Cities Soc.* **2015**. [CrossRef]
8. Luber, G.; McGeehin, M. Climate change and extreme heat events. *Am. J. Prev. Med.* **2008**, *35*, 429–435. [CrossRef] [PubMed]
9. Pantavou, K.; Theoharatos, G.; Mavrakis, A.; Santamouris, M. Evaluating thermal comfort conditions and health responses during an extremely hot summer in Athens. *Build. Environ.* **2011**, *46*, 339–344. [CrossRef]
10. Sakka, A.; Santamouris, M.; Livada, I.; Nicols, F.; Wilson, M. On the thermal performance of low income housing during heat waves. *Energy Build.* **2012**, *49*, 69–77. [CrossRef]
11. Sarrat, C.; Lemonsu, A.; Masson, V.; Guedalia, D. Impact of urban heat island on regional atmospheric pollution. *Atmos. Environ.* **2006**, *40*, 1743–1758. [CrossRef]
12. Taha, H. Meso-urban meteorological and photochemical modeling of heat island mitigation. *Atmos. Environ.* **2008**, *42*, 8795–8880. [CrossRef]
13. Rossi, F.; Bonamente, E.; Nicolini, A.; Anderini, E.; Cotana, F. A carbon footprint and energy consumption assessment methodology for UHI-affected lighting systems in built areas. *Energy Build.* **2016**, *114*, 96–103. [CrossRef]
14. Santamouris, M.; Kolokotsa, D. On the impact of urban overheating and extreme climatic conditions on housing energy comfort and environmental quality of vulnerable population in Europe. *Energy Build.* **2015**, *98*, 125–133. [CrossRef]
15. Santamouris, M. Using cool pavements as a mitigation strategy to fight urban heat island—A review of the actual developments. *Renew. Sustain. Energy Rev.* **2013**, *26*, 224–240. [CrossRef]
16. Kolokotsa, D.; Diakaki, C.; Papantoniou, S.; Vlissidis, A. Numerical and experimental analysis of cool roofs application on a laboratory building in Iraklion, Crete Greece. *Energy Build.* **2012**, *55*, 85–93. [CrossRef]
17. Kolokotsa, D.; Santamouris, M.; Zerefos, S. Green and cool roofs' urban heat island mitigation potential in European climates for office buildings under free floating conditions. *Sol. Energy* **2013**, *95*, 118–130. [CrossRef]
18. GhaffarianHoseini, A.H.; Dahlan, N.D.; Berardi, U.; Hoseini, A.G.; Makaremi, N.; Hoseini, M.G. Sustainable energy performances of green buildings: A review of current theories, implementations and challenges. *Renew. Sustain. Energy Rev.* **2013**, *25*, 1–17. [CrossRef]
19. Fahmy, M.; Sharples, S.; Yahiya, M. LAI based trees selection for mid latitude urban development: A microclimatic study in Cairo, Egypt. *Build. Environ.* **2010**, *45*, 345–357. [CrossRef]

20. Akbari, H.; Davis, S.; Dorsano, S.; Huang, J.; Winert, S. *Cooling Our Communities—A Guidebook on Tree Planting and Light Colored Surfacing*; US Environmental Protection Agency, Office of Policy Analysis, Climate Change Division: San Francisco, CA, USA, 1992.
21. Castellani, B.; Morini, E.; Filipponi, M.; Nicolini, A.; Palombo, M.; Cotana, F.; Rossi, F. Clathrate Hydrates for Thermal Energy Storage in Buildings: Overview of Proper Hydrate-Forming Compounds. *Sustainability* **2014**, *6*, 6815–6829. [CrossRef]
22. Levinson, R.; Akbari, H. Potential benefits of cool roofs on commercial buildings: Conserving energy, saving money, and reducing emission of greenhouse gases and air pollutants. *Energy Effic.* **2010**, *3*, 53–109. [CrossRef]
23. Boixo, S.; Diaz-Vicente, M.; Colmenar, A.; Castro, M.A. Potential energy savings from cool roofs in Spain and Andalusia. *Energy* **2012**, *38*, 425–438. [CrossRef]
24. Synnefa, A.; Santamouris, M.; Akbari, H. Estimating the effect of using cool coatings on energy loads and thermal comfort in residential buildings in various climatic conditions. *Energy Build.* **2007**, *39*, 1167–1174. [CrossRef]
25. Rossi, F.; Anderini, E.; Castellani, B.; Nicolini, A.; Morini, E. Integrated improvement of occupants' comfort in urban areas during outdoor events. *Build. Environ.* **2015**. [CrossRef]
26. Bonamente, E.; Rossi, F.; Coccia, V.; Pisello, A.L.; Nicolini, A.; Castellani, B.; Cotana, F.; Filipponi, M.; Morini, E.; Santamouris, M. An energy-balanced analytic model for urban heat canyons: Comparison with experimental data. *Adv. Build. Energy Res.* **2013**, *7*, 222–234. [CrossRef]
27. Rossi, F.; Cotana, F.; Filipponi, M.; Nicolini, A.; Menon, S.; Rosenfeld, A. Cool roofs as a strategy to tackle global warming: Economical and technical opportunities. *Adv. Build. Energy Res.* **2013**, *7*, 254–268. [CrossRef]
28. Akbari, H.; Menon, S. Arthur Rosenfeld. Global cooling: Increasing world-wide urban albedos to offset CO_2. *Clim. Chang.* **2009**, *95*. [CrossRef]
29. Morini, E.; Touchaei, A.G.; Castellani, B.; Rossi, F.; Cotana, F. The impact of albedo increase to mitigate the urban heat island in Terni (Italy) using the WRF model. *Sustainability* **2016**, *8*, 999. [CrossRef]
30. Touchaei, A.G.; Akbari, H. The climate effects of increasing the albedo of roofs in a cold region. *Adv. Build. Energy Res.* **2013**, *7*, 186–191. [CrossRef]
31. Mastrapostoli, E.; Karlessi, T.; Pantazaras, A.; Kolokotsa, D.; Gobakis, K.; Santamouris, M. On the cooling potential of cool roofs in cold climates: Use of cool fluorocarbon coatings to enhance the optical properties and the energy performance of industrial buildings. *Energy Build.* **2014**, *69*, 417–425. [CrossRef]
32. Yuan, J.; Emura, K.; Sakai, H.; Farnham, C.; Lu, S. Optical analysis of glass bead retro-reflective materials for urban heat island mitigation. *Sol. Energy* **2016**, *132*, 203–213. [CrossRef]
33. Meng, X.; Luo, T.; Wang, Z.; Zhang, W.; Yan, B.; Ouyang, J.; Long, E. Effect of retro-reflective materials on building indoor temperature conditions and heat flow analysis for walls. *Energy Build.* **2016**, *127*, 488–498. [CrossRef]
34. Morini, E.; Castellani, B.; Presciutti, A.; Filipponi, M.; Nicolini, A.; Rossi, F. Optic-energy performance improvement of exterior paints for buildings. *Energy Build.* **2017**, *139*, 690–701. [CrossRef]
35. Karlessi, T.; Santamouris, M. Improving the performance of thermochromic coatings with the use of UV and optical filters tested under accelerated aging conditions. *Int. J. Low-Carbon Technol.* **2015**, *10*, 45–61. [CrossRef]
36. Akbari, H.; Touchaei, A.G. Modeling and labeling heterogeneous directional reflective roofing materials. *Sol. Energy Mater. Sol. Cells* **2014**, *124*, 192–210. [CrossRef]
37. Rossi, F.; Castellani, B.; Presciutti, A.; Morini, E.; Filipponi, M.; Nicolini, A.; Santamouris, M. Retroreflective façades for urban heat island mitigation: Experimental investigation and energy evaluations. *Appl. Energy* **2015**, *145*, 8–20. [CrossRef]
38. Rossi, F.; Morini, E.; Castellani, B.; Nicolini, A.; Bonamente, E.; Anderini, E.; Cotana, F. Beneficial effects of retroreflective materials in urban canyons: Results from seasonal monitoring campaign. *J. Phys. Conf. Ser.* **2015**, *655*, 012012. [CrossRef]
39. Rossi, F.; Castellani, B.; Presciutti, A.; Morini, E.; Anderini, E.; Filipponi, M.; Nicolini, A. Experimental evaluation of urban heat island mitigation potential of retro-reflective pavement in urban canyons. *Energy Build.* **2016**, *126*, 340–352. [CrossRef]
40. Rossi, F.; Pisello, A.; Nicolini, A.; Filipponi, M.; Palombo, M. Analysis of retro-reflective surfaces for urban heat island mitigation: A new analytical model. *Appl. Energy* **2014**, *114*, 621–631. [CrossRef]

41. Aida, M. Urban Albedo as a Function of the Urban Structure-A Model Experiment. *Bound.-Layer Meteorol.* **1982**, *23*, 405–413. [CrossRef]
42. Nastasi, B.; Di Matteo, U. Solar energy technologies in Sustainable Energy Action Plans of Italian big cities. *Energy Procedia* **2016**, *101*, 1064–1071. [CrossRef]
43. Giannaros, T.M.; Melas, D.; Daglis, I.A.; Keramitsoglou, I.; Kourtidis, K. Numerical study of the urban heat island over Athens (Greece) with the WRF model. *Atmos. Environ.* **2013**, *73*, 103e111. [CrossRef]
44. Rosenzweig, C.; Solecki, W.D.; Parshall, L.; Lynn, B.; Cox, J.; Goldberg, R.; Hodges, S.; Gaffin, S.; Slosberg, R.B.; Savio, P.; et al. *Mitigating New York City's Heat Island Integrating Stakeholder Perspectives and Scientific Evaluation*; American Metheorology Society: Boston, MA, USA, 2009.
45. Papakostas, K.T.; Zagana-Papavasileiou, P.; Mavromatis, T. Analysis of 3 Decades Temperature Data for Athens and Thessaloniki, Greece—Impact of Temperature Change on Energy Consumption for Heating and Cooling of Buildings. In Proceedings of the International Conference ADAPT to CLIMATE, Nicosia, Cyprus, 27–28 March 2014; Available online: http://adapttoclimate.uest.gr/ (accessed on 14 July 2017).
46. Rosenthal, J.E.; Knowlton, K.M.; Rosenzweig, C.; Goldberg, R.; Kinney, P.L. One Hundred Years of New York City's "Urban Heat Island": Temperature Trends and Public Health Impacts. In Proceedings of the American Geophysical Union Fall Meeting, Washington, DC, USA, 8–12 December 2003.
47. 3M Italia. Available online: http://solutions.3mitalia.it/wps/portal/3M/it_IT/Window-Films/home/ (accessed on 14 July 2017).
48. Delta Ohm. Available online: http://www.otm.sg/files/LP_PYRA_05_06_uk.pdf (accessed on 14 July 2017).
49. SHIMDZU. Available online: http://www.ssi.shimadzu.com/products/product.cfm?product=solidspec (accessed on 14 July 2017).
50. American Society for Testing and Materials (ASTM). *ASTM E903–12: Standard Test Method for Solar Absorptance, Reflectance, and Transmittance of Materials Using Integrating Spheres*; ASTM International: West Conshohocken, PA, USA, 2012.
51. American Society for Testing and Materials (ASTM). *ASTM G 173–03: Standard Tables for Reference Solar Spectral Irradiances: Direct Normal and Hemispherical on 37° Tilted Surface*; ASTM International: West Conshohocken, PA, USA, 2012.
52. Adhikari, K.R.; Gurung, S.; Bhattarai, B.K. Solar Energy Potential in Nepal and Global Context. *J. Inst. Eng.* **2014**, *9*, 95–106. [CrossRef]